

Study of suitable arrangement of axial electromagnetic clutch

Ivo Doležel

Czech Technical University

166 27 Praha 6, Technická 2, e-mail: dolezel@fel.cvut.cz

Václav Kotlan, Bohus Ulrych

University of West Bohemia

306 14 Plzen, Univerzitni 26, e-mail: vkotlan@kte.zcu.cz, ulrych@kte.zcu.cz)

A methodology of designing axial magnetic clutch is presented. Except for the prescribed force, the clutch must satisfy certain requirements concerning its temperature rise and several other aspects. The methodology is illustrated by two examples.

1. Introduction

The paper deals with the design of an electromagnetic friction clutch for a combined electromagnetic-thermoelastic actuator. The task of the clutch is to fix the position of its plunger. The complete device (that is intended for an accurate setting of position [1–2]) is depicted in Fig. 1 and works in two successive steps.

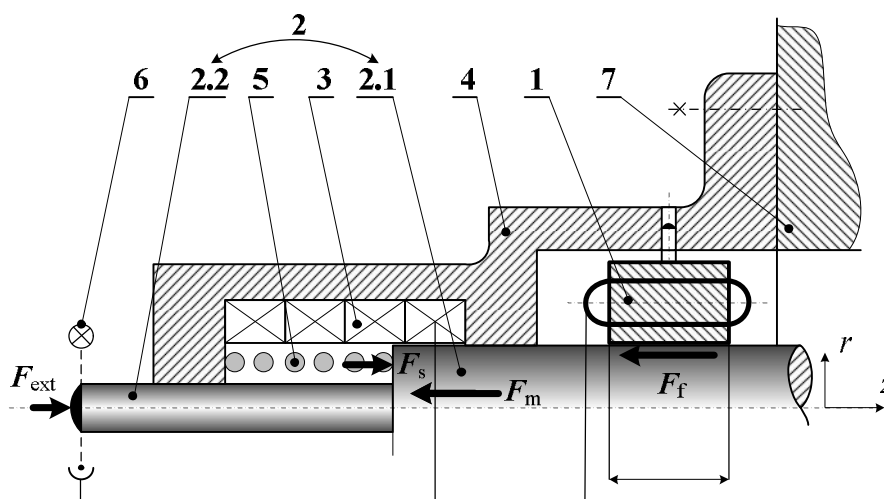


Fig. 1. A combined electromagnetic-thermoelastic actuator: 1 – friction clutch 2 – plunger (2.1 – its ferromagnetic part, 2.2 – nonferromagnetic (thermoelastic) part, 3 – field coil of the actuator consisting of several sections, 4 – shell of the actuator, 5 – return spring, 6 – photoelectric sensor of position of the plunger controlling operation of the friction clutch 1, 7 – frame of the machine

A. Electromagnetic regime

The field coil **3** (that may consist of one or rather several sections) carries direct current $I_{\text{ext,DC}}$ of density $\mathbf{J}_{\text{ext,DC}}$. This current generates in the system quasistationary magnetic field \mathbf{B}_{DC} that produces force \mathbf{F}_m acting on the ferromagnetic part **2.1** of the plunger **2**. This force pulls the plunger into the field coil **3** and must be higher than the sum of the force \mathbf{F}_s produced by the return spring **5** and possible external force \mathbf{F}_{ext} . After reaching the desired shift $\Delta u_{z,m}$ (fast, but only approximately) controlled by the photoelectric sensor **6** with wide light trace, the electromagnetic friction clutch **1** switches on, while the field coil **3** is disconnected from the DC source. Now the position of the plunger **2** is fixed, but still it may exhibit some error.

B. Thermoelastic regime

Selected sections of the coil **3** start carrying harmonic current of density $\mathbf{J}_{\text{ext,AC}}$ and frequency f that generates in the device periodic magnetic field \mathbf{B}_{AC} . This field induces in the plunger **2** (mainly in its nonferromagnetic part **2.2**) eddy currents of density \mathbf{J}_{eddy} that cause its heating and consequent dilatation $\Delta u_{z,T}$ with respect to its fixed part – friction surface of the clutch **1**. This fine dilatation is again checked by the photosensor **6**, now with narrow light trace. Even this shift may be fixed by another friction clutch (that is not present in Fig. 1).

The aim of paper is to describe and model the operation of the electromagnetic clutch **1** for massive and hollow ferromagnetic part **2.2** of the plunger.

2. Description of the device

The investigated clutch is depicted in Fig. 2. It consists of two principal parts–magnetic circuit **1** and field coil **4**. When the field coil is connected to a DC source, magnetic flux starts flowing through the magnetic circuit **1** and ferromagnetic part **3** of the plunger. This produces attractive magnetic force between these parts and its normal component in the space of jaws produces a friction force that prevents part **3** from further movement.

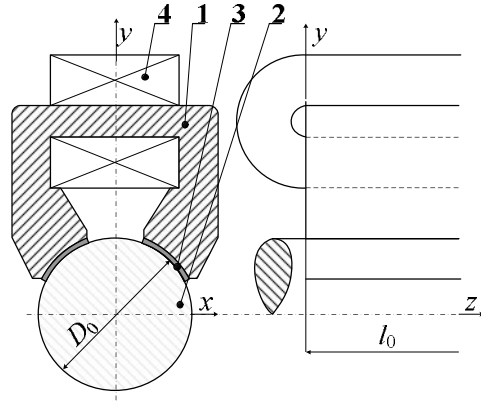


Fig. 2. Basic arrangement of the considered friction clutch: 1–ferromagnetic (carbon steel 12 040) movable frame of the clutch, 2–ferromagnetic part of the plunger whose position is to be fixed, 3–friction relining of jaws of the clutch, 4–field coil

3. Mathematical model of the pump

The mathematical model of the clutch consists of two partial differential equations describing the distribution of the magnetic and temperature fields.

The *stationary magnetic field* in the clutch is expressed in terms of the magnetic vector potential \mathbf{A} and obeys the equation [3]

$$\text{curl} \frac{1}{\mu} \text{curl} \mathbf{A} = \mathbf{J}_{\text{ext}} \quad (1)$$

where symbol μ stands for the magnetic permeability and \mathbf{J}_{ext} is the field current density. The field produces magnetic force \mathbf{F}_m acting between the magnetic circuit 1 and cylinder 2 (see Fig. 2) whose value is expressed by the integral

$$\mathbf{F}_m = \frac{1}{2} \int_S [\mathbf{H}(\mathbf{n} \cdot \mathbf{B}) + \mathbf{B}(\mathbf{n} \cdot \mathbf{H}) - \mathbf{n}(\mathbf{H} \cdot \mathbf{B})] dS \quad (2)$$

where \mathbf{H} and \mathbf{B} are vectors of the magnetic field and \mathbf{n} denotes the unit vector of the outward normal. Finally, S is the surface of the magnetic circuit 1 of the clutch.

The normal component $F_{m,n}$ of the force \mathbf{F}_m with respect to the jaws then produces the axial friction force $F_{f,a}$ between the jaws of the clutch and fixed cylinder, whose value is

$$F_{f,a} = f F_{m,n} \quad (3)$$

The *nonstationary temperature field* in the clutch is described by the equation [4]

$$\text{div}(\lambda \text{grad} T) = \rho c \frac{\partial T}{\partial t} - w_j \quad (4)$$

where λ stands for the thermal conductivity, ρ is the specific mass, c denotes the specific heat, and w_J denotes the specific ohmic losses produced by the field coil given by the formula

$$w_J = \frac{J_{\text{ext}}^2}{\gamma} \quad (5)$$

γ being the electrical conductivity of material of the coil.

4. Computer model

The numerical solution was realized using the FEM-based program QuickField (version 5.6 [5]) supplemented with a number of own procedures and scripts. The aim was to quickly obtain information about the approximate, but sufficiently accurate distributions of magnetic and temperature fields. A great attention was paid to monitoring of the convergence of solution in the dependence on some important parameters (position of the artificial boundary) and density of the discretization mesh.

After extensive testing we decided that it would be sufficient to solve a 2D model instead of a full 3D model. The error due to neglecting the front effects seems to be lower than about 8 %. In order to obtain values with three valid digits for the magnetic field, the corresponding mesh had to consist of more than 180 000 elements; for the temperature field this number could be substantially lower (as the corresponding definition area is smaller) – about 150 000 elements.

5. Illustrative examples

We present the most important results of two examples. The magnetic clutch is always the same, while in the former case the ferromagnetic part of the plunger is hollow and in the latter one massive (Fig. 3).

The principal dimensions of the friction clutch (see Figs. 2 and 3) are: $l_0 = 50$ mm, $D_0 = 30$ mm, $D_1 = 20$ mm. The magnetic circuit of the clutch as well as the ferromagnetic part of the plunger are made from carbon steel CSN 12 040. Its magnetization characteristic and temperature dependence of its important physical parameters are depicted in Figs. 4 and 5.

The field coil is made from copper, number of turns $N_c = 250$, diameter of the conductor $d = 1$ mm, factor of filling $\kappa = 0.7853$, maximum admissible temperature of insulation being $T_{\text{max}} = 200$ °C.

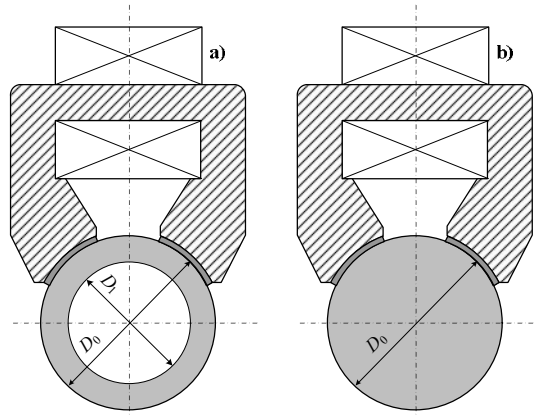


Fig. 3. Arrangement of the magnetic friction clutch: a) with hollow cylindrical ferromagnetic plunger, b) with massive cylindrical ferromagnetic plunger

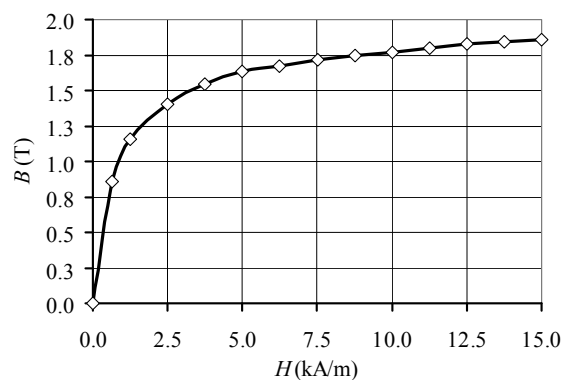


Fig. 4. Magnetization characteristic $B(H)$ of carbon steel 12 040

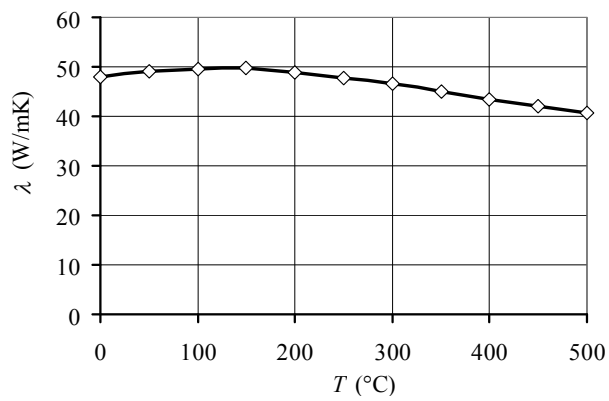


Fig. 5. Dependence $\lambda(T)$ for carbon steel 12 040

First, several figures containing results for the *hollow ferromagnetic plunger* will be presented. Figure 6 depicts the distribution of magnetic field in the system for field current of density $J_{\text{ext}} = 8 \times 10^6 \text{ A/m}^2$. In this case the upper part of the plunger is oversaturated ($B_{\text{max}} = 1.95 \text{ T}$), which deteriorates the operation parameters of the clutch – the magnetic force between the jaws and plunger decreases.

For the same value of the field current density Fig. 7 shows the distribution of the steady-state temperature field in the system. The maximum temperature of the system field coil – magnetic circuit $T_{\text{max}} = 210 \text{ }^\circ\text{C}$ occurs mainly in the field coil and neighboring parts of the yokes. But due to good thermal conductivity of carbon steel (the relining of jaws of the clutch is very thin) the temperature in the system is distributed highly uniformly and its lowest value $T_{\text{min}} = 194 \text{ }^\circ\text{C}$.

The most crucial, however, are the results that allow determining the most suitable arrangement of the clutch from the viewpoint of the friction force $F_{\text{f,a}}$. For the initial arrangement (see Fig. 3a) Fig. 8 shows the dependence of magnetic force F_{m1} (acting on one jaw of the clutch), friction force $F_{\text{f,a}}$ and maximum temperature T_{max} in the system for varying values of J_{ext} in the field coil.

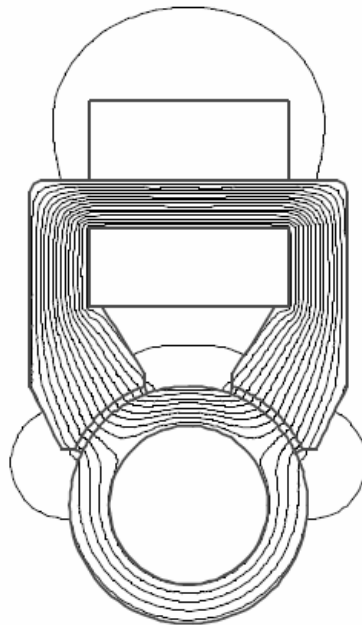


Fig. 6. Force lines of the magnetic field in the system for $J_{\text{ext}} = 8 \times 10^6 \text{ A/m}^2$
(maximum magnetic flux density in the yoke $B_{\text{max}} = 2.01 \text{ T}$)

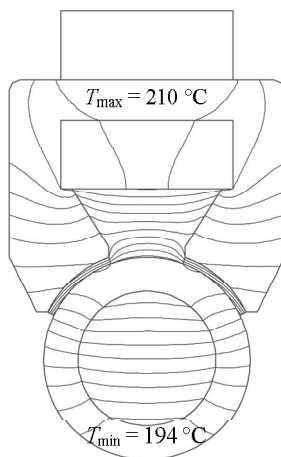


Fig. 7. Isothermal lines of the steady-state temperature field for $J_{\text{ext}} = 8 \times 10^6 \text{ A/m}^2$ (difference between neighbor isotherms $\Delta T = 0.8 \text{ }^\circ\text{C}$)

The distribution of magnetic and temperature fields for *massive ferromagnetic plunger* is quite analogous to Figs. 6 and 7. But magnetic field in the massive plunger is more uniform, which results in higher normal and friction forces. The highest and lowest temperatures in the system are somewhat lower than those in the previous case. The principal results are depicted in graphs in Fig. 9.

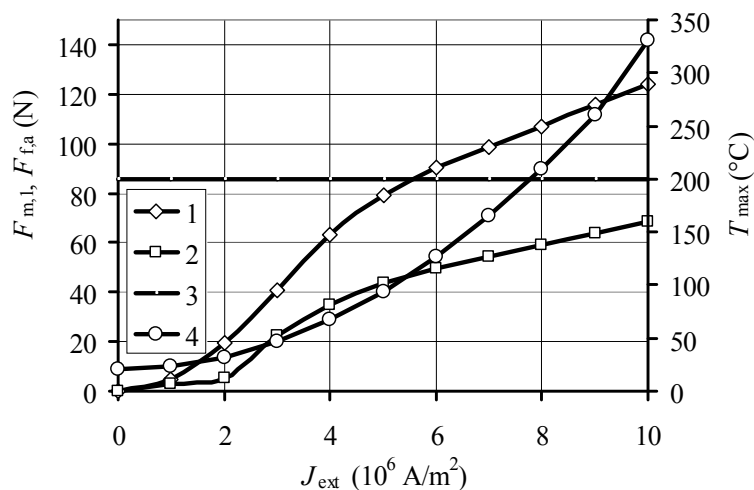


Fig. 8. Operation characteristics of the friction clutch acting on the hollow plunger (Fig. 3a),
1 – normal component of magnetic force F_{m1} acting on one jaw of the clutch, **2** – total friction force $F_{f,a}$ acting on all two jaws of the clutch, **3** – maximum acceptable temperature T_c of the field coil, **4** – actual maximum temperature T_{max} in the system

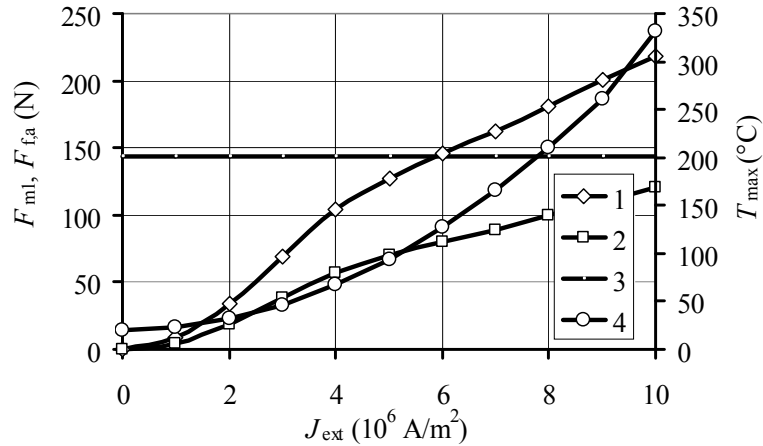


Fig. 9. Operation characteristics of the friction clutch acting on the massive plunger (Fig. 3b),
1 – normal component of magnetic force F_{m1} acting on one jaw of the clutch, **2** – total friction force $F_{f,a}$ acting on all two jaws of the clutch, **3** – maximum acceptable temperature T_c of the field coil, **4** – actual maximum temperature T_{max} in the system

6. Conclusion

The aim of the paper was to evaluate the operation parameters and characteristics of an axial magnetic clutch intended for fixing the plunger (that is partly ferromagnetic) in a combined electromagnetic-thermoelastic actuator proposed by the authors. The total friction force $F_{f,a}$ exerted by the clutch must be higher than counterforce exerted by the return spring and possible external force, as explained in paragraph 1.

In case of massive plunger the friction forces are higher due to more uniform distribution of magnetic field in the system. On the other hand, the massive plunger is heavier and higher force has to be exerted to pull it into field coil **3** of the actuator. The final decision about whether to use the hollow or massive plunger depends also on a complete economical analysis and technological possibilities of the producer.

References

- [1] Doležel, I., Ulrych, B., and Kotlan, V.: Combined electromagnetic-thermoelastic actuator for accurate setting of position. Proc. EPNC 2010, Essen, Germany, 2010, Book of abstracts.
- [2] Doležel, I., Kotlan, V., and Ulrych, B.: Electromagnetic-thermoelastic actuator for wide-range setting of position. Proc. CPEE 2010, Kynžvart, Czech Republic, 2010, CD-ROM.

I. Doležel, V. Kotlan, B. Ulrych / Study of suitable arrangement of axial...

- [3] Stratton, J. A.: Electromagnetic Theory. John Wiley & Sons, Inc., Hoboken, NJ, 2007.
- [4] Holman, J. P.: Heat Transfer. McGrawHill, New York, NY, 2001.
- [5] www.quickfield.com.

Acknowledgment

The financial support of the Grant Agency of the Czech Republic (project No. 102/09/1305), Research Plan MSM 6840770017 and project KONTAKT MEB051041 is gratefully acknowledged.